ELSEVIER

Surface Science 409 (1998) 474–484

surface science

Geometry and electronic structure of InP(001)(2×4) reconstructions

W.G. Schmidt *, F. Bechstedt

Friedrich-Schiller-Universität, Institut für Festkörpertheorie und Theoretische Optik, Max-Wien-Platz 1, 07743 Jena, Germany

Received 23 January 1998; accepted for publication 24 February 1998

Abstract

We investigate the atomic and electronic structure of the InP(001) surface by means of first-principles pseudopotential calculations within density-functional theory. We are able to rule out (4×2) reconstruction models as well as trimer configurations proposed recently as possible equilibrium structures. We predict (2×4) reconstructions characterized by asymmetric In–P or symmetric P dimers for an In-rich and a balanced surface stoichiometry, respectively. For a very limited range of preparation conditions we cannot exclude, however, the existence of further stable (2×4) reconstructions. All favourable equilibrium structures are characterized by filled and empty surface bands close to the bulk valence and conduction band edges, respectively. Details of the geometry and electronic properties for the various possible surface reconstructions are given and compared with the experimental data available.

Keywords: Density functional calculations; Indium phosphide; Molecular dynamics; Single crystal surfaces (low index single crystal surfaces)

1. Introduction

The atomic structure of the polar (001) surface of III–V compound semiconductors is relatively complicated. While the microscopic structure of GaAs(001) now seems to be well understood, there are open questions concerning the InP(001) surface. It has been claimed that ion bombardment and annealing of InP(001) result in a (4×2)/c(8×2) reconstructed, In-rich surface [1–7], in analogy to Ga-rich GaAs(001) surfaces [8]. Recently, however, this treatment has been shown to lead to a (2×4) reconstructed surface [9,10] [the authors of Ref. [9] favour an In-trimer model which corresponds to a (2×4) reconstructed surface according to the usual notation]. A (2×4) translational symmetry has also been found to result from the decapping of metal-organic vapour-phase epitaxy (MOVPE) grown samples [11,12] and from heating of the oxidized surface [13]. This agrees with the outcome of chemical-beam epitaxy [14] and molecular-beam epitaxy (MBE) experiments [15,16]. Yang and Hasegawa [17] observed a (2×4) reconstruction during gas-source MBE for both P-rich and In-rich InP(001) surfaces.

Also the reconstruction mechanism acting on InP(001) surfaces is under discussion. A wide range of atomic structures have been suggested for the surface. Based on high-resolution electron

* Corresponding author. Present address: North Carolina State University, Department of Physics, Box 8202, Raleigh, NC 27695-8202, USA. Fax: +1 919 515 7331;
e-mail: wgs@batman.physics.ncsu.edu

0039-6028/98/$19.00
PII: S0039-6028(98)00260-X

energy loss spectroscopy and ultraviolet as well as X-ray photoelectron spectroscopy, a missing-row dimer model has been proposed, where all surface In atoms are dimerized along their dangling-bond direction and one in each four rows of In atoms is missing [2–4]. A similar structure, known as $\beta 2(4\times 2)$ (Fig. 1i), is assumed to describe the ground state of the Ga-rich GaAs(001) surface [8]. The optical anisotropy of (2×4) InP surfaces, on the other hand, has been attributed to the existence of anion and cation surface dimers [15,16] in a similar way as for the $\beta 2(2\times 4)$ and α phases (Fig. 1a,b) of As-rich GaAs(001) surfaces [18–20]. In contrast to those interpretations, a series of recent studies suggests that conventional dimer models cannot explain the surface features characteristic of InP(001). On grounds of their scanning tunneling microscopy (STM) images, Shimomura et al. [7] proposed a structure which combines two In dimers in the third layer with a partial In–P exchange in the two uppermost atomic layers (Fig. 1j). MacPherson et al. [13] interpreted their STM images in terms of P-trimers (Fig. 1c). A trimerization of the topmost In atoms (Fig. 1d) has seemingly been observed in time-of-flight scattering and recoiling spectrometry by Sung et al. [9].

Previous total-energy calculations by Lewis and co-workers [21,22] are limited to (4×2) surfaces reconstructions and do not resolve the issue. In these calculations the formation of P–In–P bridge bonds (Fig. 1h) is favoured.

Less confusion exists with respect to the electronic structure of InP(001). Occupied surface states are observed to coincide roughly with the bulk valence-band maximum (VBM) [1,2,4]. An additional surface related energy band has been detected at about 1 eV below the VBM [1,4]. Empty surface states have been detected at about 1.5 eV above the VBM [1,5]. Furthermore, a strong pinning of the Fermi-level slightly below the bulk conduction-band minimum (CBM) for surfaces of both n- and p-type InP has been noted and attributed to surface defects and/or excess metallic In, rather than to states induced by the reconstruction of the clean surface [1,4].

The present study aims at clarifying the atomic structure of InP(001) in dependence on the surface stoichiometry. Based on the calculated geometries we determine the respective surface band structures and address the origin of their prominent features. To that end we perform first-principles total-energy calculations as described below.

2. Computational method

Our calculations are based on density-functional theory in local-density approximation (DFT-

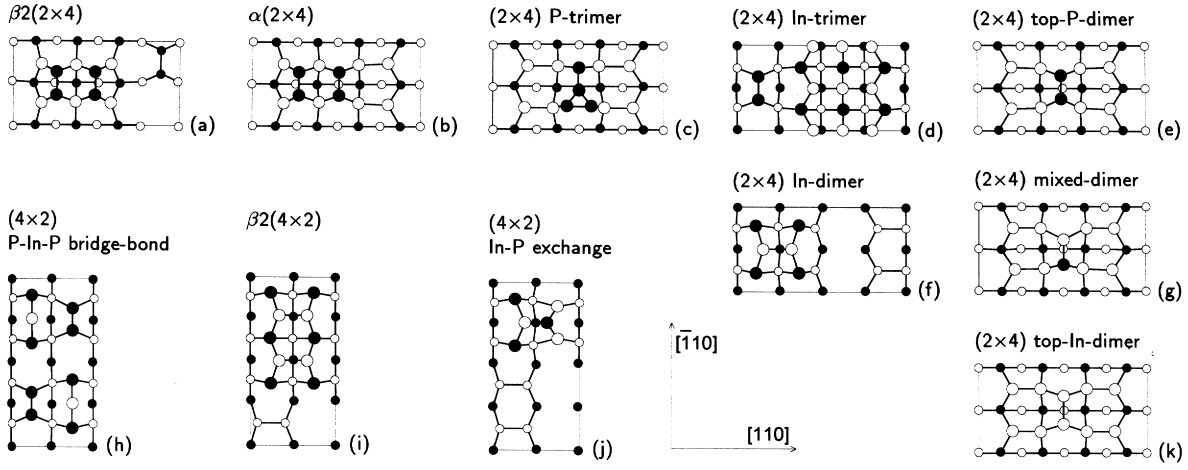

Fig. 1. Top view of InP(001)(2×4) and (4×2) surface reconstruction models ordered with increasing In coverage. Empty (filled) circles represent In (P) atoms. Large (small) symbols indicate positions in the first and second (third and fourth) atomic layers.

LDA). We consider an artificial periodic slab geometry along the surface normal. The unit cell includes an atomic slab with seven (eight) atomic InP(001) layers for cation (anion) terminated surfaces and a vacuum region equivalent in thickness. The cation terminated bottom layer of the slab is saturated with fractionally ($Z=1.25$) charged H atoms [23]. Two layers on this side of the slab are kept frozen, whereas all other atoms are allowed to relax. The electric field resulting from the inequivalence of the two surfaces is accounted for by a dipole correction to the electrostatic potential calculated self-consistently. The electron–ion interaction is treated by using fully separable, norm-conserving pseudopotentials [24]. For the many-body electron–electron interaction we employ the exchange and correlation potential by Ceperley and Alder [25]. Single-particle orbitals are expanded into plane waves up to an energy cut-off of 15 Ry. $\boldsymbol{k}$-Space integrations are replaced by a sum over four special points in the irreducible part of the surface Brillouin zone. The minimum of the total-energy functional with respect to both the electronic and atomic degrees of freedom is found by means of a molecular–dynamical approach [26,27]. The atoms are assumed to be in their fully relaxed positions when the forces acting on the ions are smaller than 0.025 eV/Å. The calculations are performed with the theoretical equilibrium lattice constant of 5.67 Å, which is smaller than the measured value of 5.87 Å. This discrepancy is mainly attributed to the missing contribution of the In 4d states, which are considered as frozen-core states and therefore hidden in the pseudopotential. Our approach and numerical parameters have proven reliable in determining the structural [28] and dynamical properties [29] of the InP(110) surface. The calculations are on the same footing as a recent study on GaAs(001) [19,20].

3. Results

3.1. Surface phase diagram

We perform total-energy calculations for 11 structural models for (2×4) and (4×2) reconstructed InP(001) surfaces. These comprise geometries suggested in the past for InP(001) (Fig. 1c,d,h,j) [7,9,13,21,22], structures which are assumed to exist on GaAs(001) (Fig. 1a,b,i) [8,18–20] as well as four models which seem to be consistent with the outcome of recent STM measurements and soft X-ray photoelectron spectroscopy (SXPS) [11,12] as will be explained below (Fig. 1e,f,g,k). The 11 structures realize different In coverages of $\Theta=1/4$ [$\beta2(2\times4)$, P–In–P bridge-bond], $\Theta=1/2$ (α, P-trimer), $\Theta=3/4$ [$\beta2(4\times2)$, In-trimer, In-dimer, top-P-dimer], $\Theta=1$ (In–P exchange, mixed-dimer) and $\Theta=5/4$ (top-In-dimer). Therefore, an energetic comparison of these structures can only be made by taking into account the chemical potentials of the surface constituents In and P. The ground state of the surface is determined by the minimum of the grand canonical thermodynamic potential:

$$\Omega = U - TS - \sum_{\mathrm{X}} \mu(\mathrm{X}) n_{\mathrm{X}} \tag{1}$$

where U is the total energy of the system. The entropy term, TS, contributes very little to the difference in Ω for various structures under the usual experimental conditions, and is neglected (for a more detailed discussion, see e.g. Refs. [30,31]). n_{X} denotes the number of particles of the respective species X = In, P. The chemical potentials $\mu(\mathrm{X})$ are restricted by:

$$\mu(\mathrm{X}) \le \mu(\mathrm{X})_{\mathrm{bulk}} \tag{2}$$

Furthermore, they are related to each other by:

$$\mu(\mathrm{In}) + \mu(\mathrm{P}) = \mu(\mathrm{InP})_{\mathrm{bulk}} = \mu(\mathrm{In})_{\mathrm{bulk}} + \mu(\mathrm{P})_{\mathrm{bulk}} - \Delta H_{\mathrm{f}}(\mathrm{InP}) \tag{3}$$

with $\Delta H_{\mathrm{f}}(\mathrm{InP})$ being the heat of formation of InP. Consequently, the formation energy may be written as a function of a single variable, which we will take to be $\Delta\mu(\mathrm{In}) := \mu(\mathrm{In}) - \mu(\mathrm{In})_{\mathrm{bulk}}$ with:

$$-\Delta H_{\mathrm{f}}(\mathrm{InP}) \le \Delta\mu(\mathrm{In}) \le 0 \tag{4}$$

where $\mu(\mathrm{In})_{\mathrm{bulk}}$ has been determined from a calculation of bulk indium. Thereby the lattice constant was optimized with respect to the total energy. For $\Delta H_{\mathrm{f}}(\mathrm{InP})$ we take the experimental value of 0.92 eV [32]. Thus we are able to limit the thermodynamically allowed range of the surface chemical

potentials with an accuracy of a few tenths of one electronvolt [33]. Now we can determine the ground state of the surface for the different preparation conditions between the limits of extreme In-poor (P-rich) and In-rich (P-poor) surfaces. In Fig. 2 we show the calculated surface phase diagram versus the In chemical potential.

For both P- and In-rich surfaces we find the ground state of InP(001) to be (2×4) reconstructed. This is in contrast to the Ga-stabilized GaAs(001) surface [8,18,33]. The most favourable (4×2) reconstruction, the InP(001)$\beta2(4\times2)$ structure is about 0.14 eV per surface atom higher in energy than the (2×4) top-P-dimer model. Therefore it can safely be excluded as an equilibrium structure. It is interesting to note that the only model which does not satisfy electron counting heuristics [34], namely the P–In–P bridge-bond model [21,22], is among the most unfavourable geometries. This indicates the validity of the electron counting rule also for InP(001) surfaces.

The trimer-like surface structures suggested by Sung et al. [9] and MacPherson et al. [13] as well as the In–P exchange seemingly observed by Shimomura et al. [7] are higher in energy than dimer reconstruction models. Our calculations favour for In-rich surfaces the formation of mixed In–P dimers on top of an In-terminated surface (Fig. 1g). For less In-rich surfaces the $\beta2(2\times4)$ reconstruction adapted from As-rich GaAs surfaces [18–20] represents the surface ground state. This agrees with the experimental observation of two different (2×4) phases [15–17]. On grounds of measurements of the surface optical anisotropy, the two surface phases were hypothesized to be dominated by [110]-oriented In–In and $[\bar{1}10]$-orientated P–P bonds for the high and low temperature regime, respectively [15,16]. This hypothesis is corroborated by the present calculations, which favour the mixed-dimer model containing four In–In bonds for In-rich surfaces and the $\beta2(2\times4)$ phase featuring three P–P dimers for less In-rich conditions. Taking the limited accuracy of our calculations into account, we cannot exclude, however, the existence of further surface structures for a very narrow range of preparation conditions. The $\alpha(2\times4)$ phase and/or the top-P-dimer geometry may occur for intermediate values of the In chemical potential. For values $\Delta\mu(\mathrm{In})\approx-1/3\Delta H_f(\mathrm{InP})$ even a coexistence of several (2×4) reconstructed surface structures might be observed. This could be one explanation for the varying findings of different experimental groups concerning the ground state geometry of InP(001) as discussed in the Introduction.

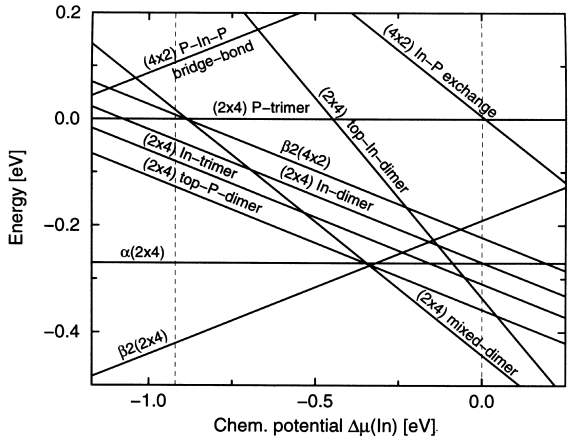

Fig. 2. Relative formation energy (with respect to the P-trimer structure) per (1×1) unit cell for InP(001) surface reconstructions vs. $\Delta\mu(\mathrm{In})$. The thermodynamically allowed range is indicated by dashed lines.

For P-rich surfaces, on the other hand, (2×1), (2×2) and $c(4\times4)$ RHEED patterns have been observed [15,16]. Therefore, geometries different from those studied here are probably favoured for P-rich surfaces.

3.2. Geometry and bonding

Structural details of the energetically favoured surface structures are given in Table 1 (cf. Fig. 3). They are all characterized by first-layer dimers [and third-layer dimers in case of the $\beta2(2\times4)$ structure] parallel to the $[\bar{1}10]$ direction. In–In bonds in the second atomic layer form along the [110] direction in case of the mixed-dimer, top-P-dimer and α structures.

The most striking feature of the mixed-dimer model, favoured for In-rich surfaces, is the asymmetric topmost In–P dimer with a buckling of $\Delta_{a,\perp}=0.46$ Å. The uppermost In atom assumes a nearly planar, sp^2-like bonding configuration while the uppermost P atom forms nearly right-angled

Table 1
Geometrical parameters (Å) of energetically favoured structural models for the InP(001)(2×4) surface (cf. Fig. 3)

InP(001)(2×4)	Mixed-dimer	β2	Top-P-dimer	α
$\Delta_{a1,x}$	2.40	2.21	2.22	2.22
$\Delta_{a2,x}$	—	—	—	2.22
$\Delta_{b1,x}$	3.96	3.71	3.95	3.94
$\Delta_{b2,x}$	3.85	3.52	3.71	3.68
$\Delta_{b3,x}$	—	—	—	3.51
$\Delta_{b4,x}$	—	—	—	3.73
$\Delta_{c,x}$	—	2.25	—	—
$\Delta_{d,x}$	—	3.74	—	—
$\Delta_{a,y}$	—	3.71	—	3.85
$\Delta_{b,y}$	2.84	—	2.84	2.82
$\Delta_{b',y}$	2.67	—	—	—
$d_{ab,y}$	1.85	1.49	1.89	1.47
$d_{ab',y}$	2.22	—	—	1.83
$\Delta_{a,\perp}$	0.46	—	—	0.09
$\Delta_{b12,\perp}$	0.30	0.18	0.22	0.21
$\Delta_{b23,\perp}$	—	—	—	0.05
$\Delta_{b34,\perp}$	—	—	—	0.19
$d_{ab,\perp}$	1.08	1.55	1.50	1.44

bonds to the In atoms below. This bonding behaviour of cations and anions is typical for surfaces of III–V compound semiconductors [18–20,28,33]. The In–P bond length of the mixed dimer is 2.44 Å, rather close to the ideal bulk bond length of 2.46 Å. The mixed-dimer model combines the structural features proposed on grounds of STM studies: The formation of In–P bonds in the first atomic layer has been suggested by Shimomura et al. [7], whereas the formation of In–In bonds in the second atomic layer has been hypothesized by MacPherson et al. [13]. We mention that the domain boundaries observed by STM [7,13], which cannot be explained by dimer reconstruction models known from GaAs(001), may easily be constructed by means of asymmetric single dimer units. Finally, the existence of just one dimer in the top atomic layer may explain the appearance of rather narrow protrusions observed by STM [11] on In-rich surfaces. Due to the different three- and four-fold coordinations of the second-layer cations, we observe a buckling $\Delta_{b12,\perp}$ of the In–In bonds of 0.30 Å on average. The occurrence of two differently bonded surface cations gives a natural explanation for the SXPS finding of two In 4d surface components [12]. The In 4d signal at higher binding energy is most likely due to the charge transfer from the three-fold coordinated In to the three-fold coordinated P surface atoms as postulated by the electron counting rule [34]. The low binding energy surface component of In 4d is probably due to the four-fold coordinated surface In atoms, which are characterized by a relative charge accumulation with respect to the bulk indium surrounded by phosphorus.

The InP(001)β2(2×4) surface structure is similar to the corresponding geometry of As-rich GaAs(001) surfaces [19,20]. The topmost dimers are nearly symmetric, while a small buckling of 0.02 Å (GaAs: 0.05 Å) occurs for the anion dimer in the third atomic layer. The P–P dimer lengths are 2.21 and 2.25 Å in the first and third atomic layers, respectively. The dimer lengths are thus about 5.2% (GaAs: 4.6%) longer than the sum of the anion covalent radii. These slight differences between structural details of GaAs and InP surfaces are due to the larger size difference between cations and anions in case of InP. The three-fold coordinated second-layer In atoms bonded to P dimer atoms prefer a nearly planar, sp^2-like bonding situation. They are displaced from their ideal lateral position by about 0.68 Å towards the P dimers. This leads to an upward movement of the P dimers with respect to the ideal lattice. We find the minimum interplanar distance $d_{ab,\perp}$ between the first and second layers to be 1.55 Å, about 9% larger than the bulk spacing. The bond length between the three-fold coordinated In atoms and the P dimer atoms is 2.40 Å, about 2.2% shorter than the ideal bulk bond length. The latter value is, however, essentially preserved in the bonds between the P dimer atoms and the four-fold coordinated cations below. Such a bimodal bond length distribution between top-layer anions and second-layer cations has also been found for GaAs(001) surfaces [19,20,35].

Similar structural motifs characterize the top-P-dimer and the α model, which may occur for a very narrow range of preparation conditions. Both models have symmetric P dimers with a length of 2.22 Å in the uppermost atomic layer and strong In–In bonds in the second atomic layer (bond length 2.83–2.86 Å). As discussed for the previous structures, three-fold coordinated cations assume a nearly planar bonding configuration.

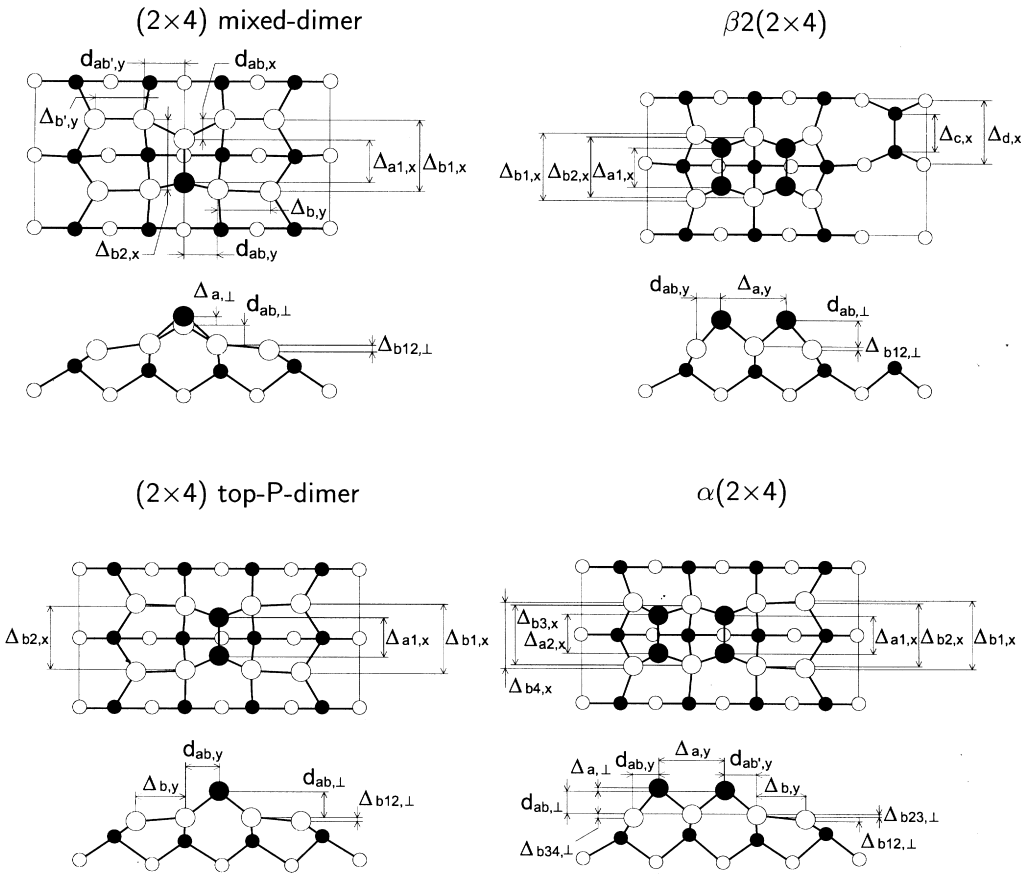

Fig. 3. Top and side view of energetically favoured InP(001)(2×4) surface reconstruction models. Empty (filled) circles represent In (P) atoms. Large (small) symbols indicate positions in the first and second (third and fourth) atomic layers.

For extreme cation-rich GaAs(001) surfaces a β2(4×2) reconstruction occurs [8,18,33] (Fig. 1i), where three surface cation dimers orientated along [110] form the (4×2) surface unit cell. Such a structure is energetically unfavourable for InP(001) surfaces as shown in Fig. 2. This may be understood as a consequence of the larger size difference between anions and cations in case of InP. The ratio of the covalent radii of In and P is about 1.36, while it amounts only to 1.05 for Ga and As [36]. This size difference hinders the accommodation of sp^2-hybridized In-dimer atoms at the surface due to an appreciable stress in the subsurface layers caused by the three-fold coordinated cations. At the GaAs(001)β2(4×2) surface the Ga dimer atoms form bond angles of about 143° with the second layer anions [33], whereas these angles amount only to about 117° for InP(001)β2(4×2). The latter value is much less favourable for sp^2-hybridization. The mixed-dimer model, on the other hand, allows the formation of strong In–In bonds (bond lengths 2.7–2.9 Å), while, due to the fact that four surface In atoms remain four-fold coordinated and near their ideal positions, the surface stress is low. The same arguments hold in case of α and top-P-dimer structures, which may occur for a small range of preparation conditions.

3.3. Electronic properties

The discussion of the electronic properties of the InP(001)(2×4) surface focuses on the most favourable reconstruction models.

In Fig. 4 the bound surface state energy bands of the mixed-dimer model are shown together with the projected InP bulk band structure. The surface is semiconducting. All occupied surface bands are below the bulk VBM. V1, the highest occupied surface band, has its maximum at the J′ point, 0.1 eV below the bulk valence band edge. This surface band is related to σ-like bonds between the topmost In atom and the two In atoms below (cf. Fig. 5). V2, 0.4 eV below the bulk VBM at K, is the surface band related to the P dangling bond at the topmost P atom. Together with the electron distribution in the wave functions related to V1, the V2 orbitals may explain the triangular shape of the corrugations observed in the STM images taken at negative bias voltages of −1.5 V [7,13]. The lateral positions of the resulting three maxima in the electron distribution due to V1 and V2 form an isosceles triangle (cf. Fig. 5). Other surface states will also contribute to the observed STM images. These states, however, possess maxima of the probability below the top dimer atoms. This is illustrated for the V3 state in Fig. 5, where the corresponding probability density is shown in a plane 1.2 Å below the top P atoms. At K the corresponding band energy is found about 0.5 eV below the bulk valence-band edge. V3 arises from σ-type bonds between the second layer In atoms close to the uppermost P atom. The unoccupied surface state bands of the mixed-dimer model extend into the bulk band gap, in particular near Γ in the surface Brillouin zone. The lowest unoccupied surface bands, C1–C4, are mainly due to dangling bonds at the three-fold coordinated In atoms in the second atomic layer. At about 2.2 eV above the bulk VBM we find the σ*-like antibonding combination of an sp^2-hybrid at the topmost In atom and a p-like orbital at the top P atom. The corresponding bonding combination of the mixed In–P dimer gives rise to a surface resonance within the InP valence band at about 0.9 eV below the bulk VBM. Because of the problematic identification of resonant surface states in slab calculations, we have not mapped the corresponding bands.

Also, in case of the InP(001)β2(2×4) structure all occupied surface bands lie below the bulk valence-band edge (cf. Fig. 6). The highest occupied surface band, V1 assumes its maximum at the K point, 0.2 eV below the bulk valence band edge.

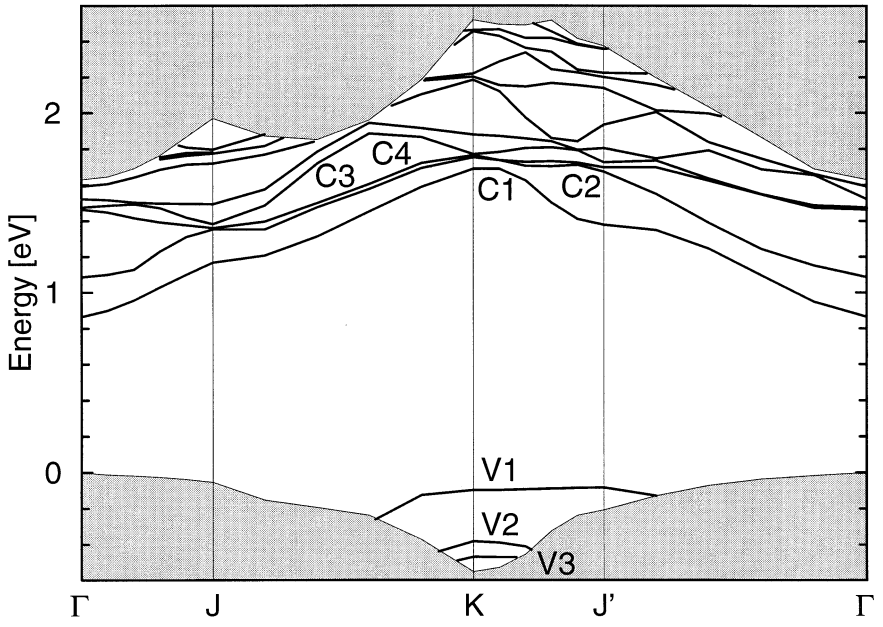

Fig. 4. Surface band structure (bound states) for the mixed-dimer model of the InP(001)(2×4) surface. Grey regions indicate the projected bulk band structure.

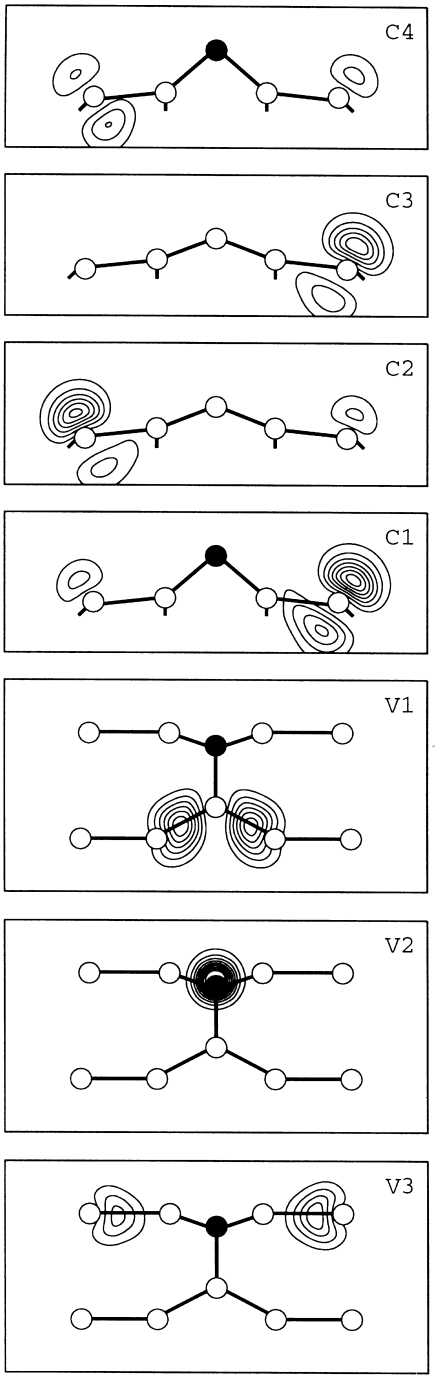

Fig. 5. Contour plots of the squared wave functions at K for surface localized states of the mixed-dimer model of the InP(001)(2×4) surface. The contour spacing is 10^{-3} e bohr^{-3}. The notation of the states refers to Fig. 4. Top views with projection planes 0.8 Å below, 0.8 Å above and 1.2 Å below the uppermost P atom show the occupied states V1, V2 and V3. The plots for the empty surface states C1–C4 are drawn in ($\bar{1}$10) planes cutting the bonds between first- and second-layer atoms.

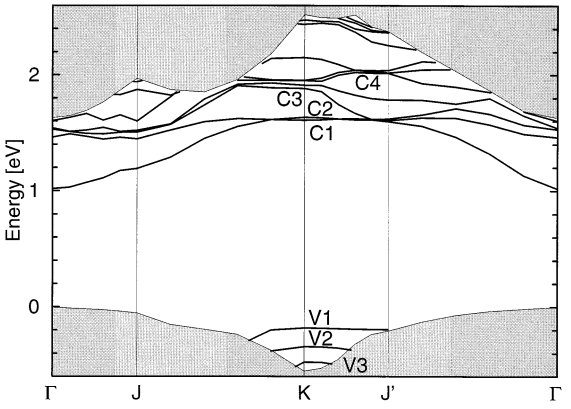

Fig. 6. Surface band structure (bound states) for the InP(001)β2(2×4) surface. Grey regions indicate the projected bulk band structure.

This only weakly dispersive feature corresponds to an anti-bonding π* combination of p_z orbitals localized at the third-layer P dimer (cf. Fig. 7). The energetical position and orbital character of this state are comparable to the highest occupied surface state at the GaAs(001)β2(2×4) surface [19,20]. Similarities to the case of GaAs are also observed for the energetically lower lying bands V2 and V3, 0.3 and 0.5 eV below the VBM at K, respectively. They arise from an anti-bonding π* combination of p_z orbitals localized at the topmost P dimers and from σ-type bonds between the top P dimer atoms and the In atoms below. In contrast to the case of GaAs, we do not find, however, bound surface states due to the π bonding combinations of the P dimers in the same energy region. This is most probably related to the much shorter anion dimer length in case of InP, which causes a stronger π/π* splitting. The stronger splitting may also explain the similar energetic positions of the highest surface valence states in spite of the different orbital energies of P 2p and As 3p electrons (−9.54 and −8.98 eV, respectively [37]). Further differences of the electronic structure of the β2(2×4) phases of (001) surfaces of InP and

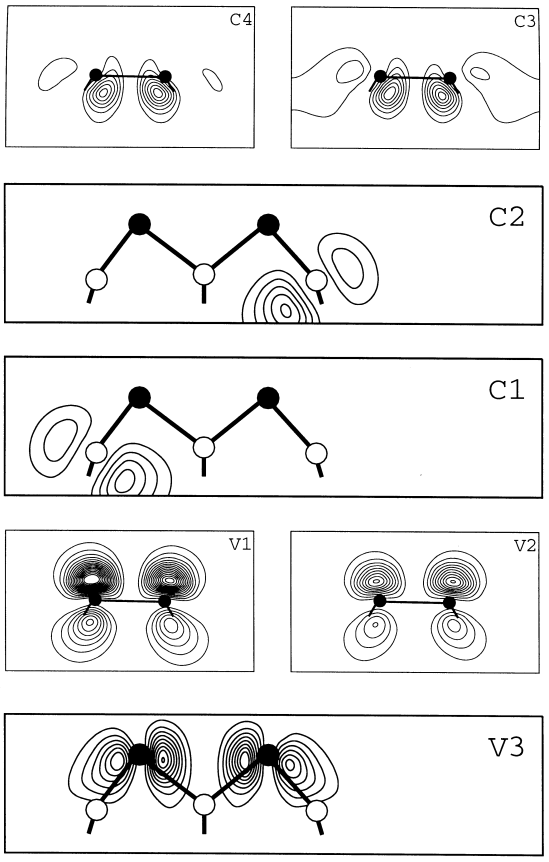

Fig. 7. Contour plots of the squared wave functions at K for surface localized states of the InP(001)β2(2×4) surface. The contour spacing is 10^{-3} e bohr^{-3}. The notation of the states refers to Fig. 6. All plots are drawn parallel to the surface normal. C4 and V2 are localized at the two topmost P dimers, C3 and V1 are localized at the third layer P dimer. C2, C1 and V3 are plotted along a $(\bar{1}10)$ plane cutting the bonds between first-layer anions and second-layer cations.

GaAs concern the unoccupied states. These states are essentially above the bulk conduction band edge for GaAs(001). For InP, however, they extend significantly into the region of the fundamental gap in the ***k***-space region around Γ. The lowest unoccupied states, C1 and C2, are related to empty dangling bonds located at the three-fold coordinated second-layer In atoms. C3 and C4 are anti-bonding σ* combinations of in-plane p orbitals at the third-layer and top-layer P dimers, respectively.

In Figs. 8 and 9 we show the calculated surface

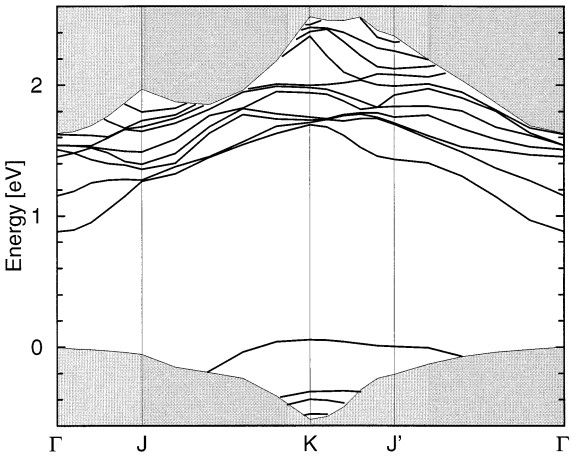

Fig. 8. Surface band structure (bound states) for the top-P-dimer model of the reconstructed (2×4) surface. Grey regions indicate the projected bulk band structure.

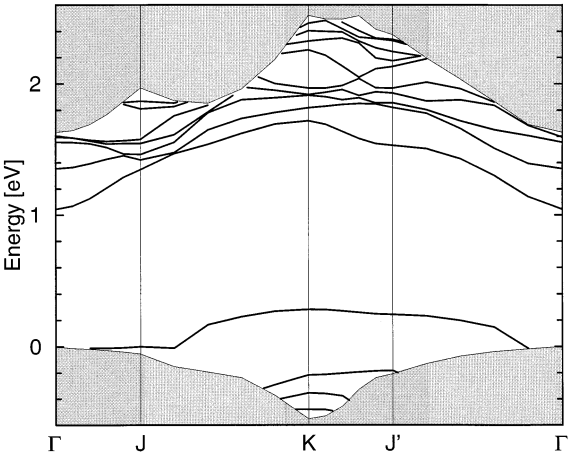

Fig. 9. Surface band structure (bound states) for the InP(001)α(2×4) surface. Grey regions indicate the projected bulk band structure.

bands of the top-P-dimer model and the α(2×4) phase of the InP(001) surface. In contrast to the mixed-dimer model and the β2(2×4) phase discussed above, we notice some extension of occupied surface states into the energy region of the fundamental gap. The highest occupied surface band of the top-P-dimer model assumes its maximum at the K point 0.1 eV above the bulk VBM. This band is due to an anti-bonding π* combination of p_z orbitals localized at the topmost P dimer.

Even larger (0.3 eV) is the extension of occupied states in the bulk band gap in case of the α structure. We find the onset of the unoccupied surface states to lie below the bulk conduction-band edge for both the top-P-dimer model and the $\alpha(2\times4)$ phase.

The band structures presented here suffer from the well-known DFT-LDA gap problem, i.e. underestimated excitation energies. The inclusion of many-body effects related to the particle excitation leads to a considerable improvement. In particular, empty surface states are shifted more than empty bulk states towards higher energies [38,39]. On the other hand, the underestimation of the equilibrium lattice constant and the neglect of the relaxation of the In 4d electrons in our calculation lead to a widening of the fundamental gap. This overcompensates the underestimation of the excitation energies within DFT-LDA at least for the direct gap at Γ. Nevertheless, we expect the unoccupied surface states to change somewhat their position with respect to the projected bulk band structure. Our results concerning the surface band structures agree roughly with the experimental findings [1,2,4,5] discussed in the Introduction, provided that there is indeed a shift of the unoccupied surface bands towards higher energies.

The self-consistently calculated potential sensed by the electrons in the slabs containing the specific surface structures allows us to determine the energy barrier for an electron passing from the bulk to the vacuum region [40]. The ionization energy I corresponds to the difference between this potential in the vacuum region and the VBM. For the P-rich InP(001)$\beta2(2\times4)$ surface we calculate a value $I=$ 5.3 eV. The ionization energy decreases gradually with increasing In coverage (cf. Fig. 10). The reduction of the ionization energy can be explained by the formation of a surface dipole between surface anions and cations. The values obtained for the In-rich top-P-dimer structure ($I=4.6$ eV) and the mixed-dimer model ($I=4.52$ eV) agree well with experimental findings of 4.5 ± 0.15 eV [5] and 4.61 eV [41]. This agreement between calculated and measured ionization energies may be somewhat fortuitous. It indicates, however, the validity of the structural models suggested here for In-rich surfaces. For higher In coverages the ionization energy should approach the work function value of 4.12 eV of metallic In [32].

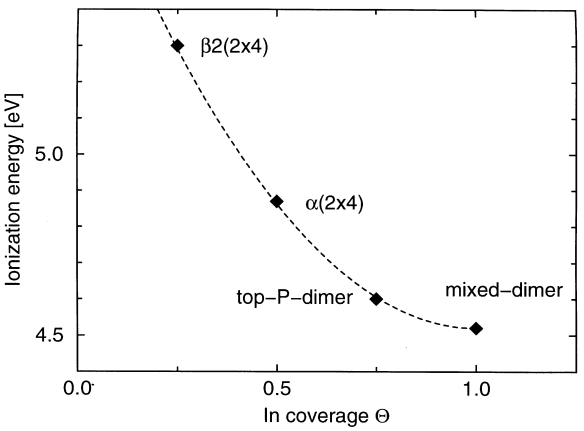

Fig. 10. Calculated ionization energy vs. coverage for four energetically favoured surface structures. The dashed line is to guide the eye. It represents the function $I=[4.52+1.37(\Theta-1)^2]$ eV.

4. Conclusions

In conclusion, we have presented a comprehensive study of the atomic structure and electronic properties of (2×4) and (4×2) reconstructions of InP(001). For both a balanced surface stoichiometry and for In-rich conditions we favour a (2×4) reconstructed surface which is stabilized by the formation of dimers. The microscopic structure of the cation-rich surface differs from the well-investigated GaAs(001) surface due to the remarkable size difference between cations and anions in case of InP. All possible equilibrium structures are characterized by semiconducting surfaces in accordance with electron counting heuristics.

Acknowledgements

Financial support by the Deutsche Forschungsgemeinschaft under Project Be 1346/6-2 is gratefully acknowledged.

References

[1] J.M. Moison, M. Bensoussan, Surf. Sci. 168 (1986) 68.
[2] X. Hou, G. Dong, X. Ding, X. Wang, J. Phys. C: Solid State Phys. 20 (1987) L121.
[3] X. Wang, Appl. Surf. Sci. 33/34 (1988) 88.
[4] W. Weiss, R. Hornstein, D. Schmeisser, W. Göpel, J. Vac. Sci. Technol. B8 (1990) 715.
[5] S. Riese, E. Milas, H. Merz, Surf. Sci. 269/270 (1992) 833.
[6] J. Woll, Th. Allinger, V. Plyakov, J.A. Schaefer, A. Goldmann, W. Erfurth, Surf. Sci. 315 (1994) 293.
[7] M. Shimomura, N. Sanada, Y. Fukuda, P.J. Moller, Surf. Sci. 359 (1996) L451.
[8] D.K. Biegelsen, R.D. Bringans, J.E. Northrup, L.-E. Swartz, Phys. Rev. 41 (1990) 5701.
[9] M.M. Sung, C. Kim, H. Bu, D.S. Karpuzov, J.W. Rabelais, Surf. Sci. 322 (1995) 116.
[10] D. Pahlke, J. Kinsky, Ch. Schultz, M. Pristovsek, M. Zorn, N. Esser, W. Richter, Phys. Rev. B 56 (1997) R1661.
[11] N. Esser, U. Resch-Esser, M. Pristovsek, W. Richter, Phys. Rev. B 53 (1996) R13257.
[12] W.G. Schmidt, F. Bechstedt, N. Esser, M. Pristovsek, Ch. Schultz, W. Richter, Phys. Rev. B, in press.
[13] C.D. MacPherson, R.A. Wolkow, C.E.J. Mitchell, A.B. McLean, Phys. Rev. Lett. 77 (1996) 691.
[14] B. Junno, S. Jeppesen, M.S. Miller, L. Samuelson, J. Cryst. Growth 164 (1996) 66.
[15] K.B. Ozanyan, P.J. Parbrook, M. Hopkinson, C.R. Whitehouse, Z. Sobiesierski, D.I. Westwood, J. Appl. Phys. 82 (1997) 474.
[16] P.J. Parbrook, K.B. Ozanyan, M. Hopkinson, C.R. Whitehouse, Z. Sobiesierski, D.I. Westwood, Appl. Surf. Sci. 123/124 (1998) 313.
[17] B.X. Yang, H. Hasegawa, Jpn. J. Appl. Phys. 33 (1994) 742.
[18] J.E. Northrup, S. Froyen, Mater. Sci. Eng. B30 (1995) 81.
[19] W.G. Schmidt, F. Bechstedt, Phys. Rev. B 54 (1996) 16742.
[20] W.G. Schmidt, F. Bechstedt, Surf. Sci. 360 (1996) L473.
[21] J.-M. Jin, L.J. Lewis, Surf. Sci. 325 (1995) 251.
[22] H. Seong, L.J. Lewis, Surf. Sci. 337 (1995) 166.
[23] K. Shiraishi, J. Phys. Soc. Jpn. 59 (1990) 3455.
[24] X. Gonze, R. Stumpf, M. Scheffler, Phys. Rev. B 44 (1991) 8503.
[25] D.M. Ceperley, B.J. Alder, Phys. Rev. Lett. 45 (1980) 566.
[26] R. Car, M. Parrinello, Phys. Rev. Lett. 55 (1985) 2471.
[27] R. Stumpf, M. Scheffler, Comput. Phys. Commun. 79 (1994) 447.
[28] J.L.A. Alves, J. Hebenstreit, M. Scheffler, Phys. Rev. B 44 (1991) 6188.
[29] W.G. Schmidt, F. Bechstedt, G.P. Srivastava, Phys. Rev. B 52 (1995) 2001.
[30] G.-X. Qian, R.M. Martin, D.J. Chadi, Phys. Rev. Lett. 60 (1988) 1962.
[31] G.-X. Qian, R.M. Martin, D.J. Chadi, Phys. Rev. B 38 (1988) 7649.
[32] D.R. Lide (Ed.), CRC Handbook of Chemistry and Physics, CRC Press, Boca Raton, FL, 77th edn., 1996.
[33] W.G. Schmidt, Appl. Phys. A65 (1997) 581.
[34] M.D. Pashley, Phys. Rev. B 40 (1989) 10481.
[35] G.P. Srivastava, S. Jenkins, Phys. Rev. B 53 (1996) 12589.
[36] Table of Periodic Properties of the Elements, Sargent-Welch Scientific, Skokie, IL, 1980.
[37] C.F. Fischer, Atom. Data 4 (1972) 301.
[38] F. Bechstedt, R. Del Sole, Solid State Commun. 74 (1990) 41.
[39] C. Kress, M. Fiedler, W.G. Schmidt, F. Bechstedt, Phys. Rev. B 50 (1994) 17697.
[40] F. Bechstedt, M. Scheffler, Surf. Sci. Rep. 18 (1993) 145.
[41] K.-H. Chang, P. Meijer, J. Vac. Sci. Technol. 14 (1977) 789.